

1      Supplementary Information for Intensified Diurnal Cycle of  
2      Convection Explains Half of Tropical High-Cloud Feedback

3      Jakob Deutloff<sup>1, 2, 3\*</sup>, Stefan A. Buehler<sup>1, 2</sup>, Julia Windmiller<sup>4</sup>,  
4      Ann Kristin Naumann<sup>5</sup>

5      <sup>1</sup>\*Earth System Sciences, Atmospheric Science, University of Hamburg, Hamburg, Germany.

6      <sup>2</sup>Earth and Society Research Hub (ESRAH), Hamburg, Germany.

7      <sup>3</sup>International Max Planck Research School on Earth System Modelling (IMPRS-ESM),  
8      Hamburg, Germany.

9      <sup>4</sup>Max Planck Institute for Meteorology, Hamburg, Germany.

10     <sup>5</sup>Ludwig-Maximilians-Universität in Munich, Munich, Germany.

11     \*Corresponding author(s). E-mail(s): [jakob.deutloff@uni-hamburg.de](mailto:jakob.deutloff@uni-hamburg.de);

12     Contributing authors: [stefan.buehler@uni-hamburg.de](mailto:stefan.buehler@uni-hamburg.de); [julia.windmiller@mpimet.mpg.de](mailto:julia.windmiller@mpimet.mpg.de);  
13     [a.naumann@lmu.de](mailto:a.naumann@lmu.de);

<sup>14</sup> **S1 Influence of Time of Occurrence on High-Cloud Radiative Effect**

<sup>15</sup> The SW  $C(I)$  becomes stronger for more incoming solar radiation, which can be modulated by the local  
<sup>16</sup> time at which the respective cloud occurs, and its distance to the equator. To first order, the incoming  
<sup>17</sup> SW radiation is governed by the timing of the clouds. This becomes evident by the solar radiation closely  
<sup>18</sup> following the time difference to noon (Fig. S1).

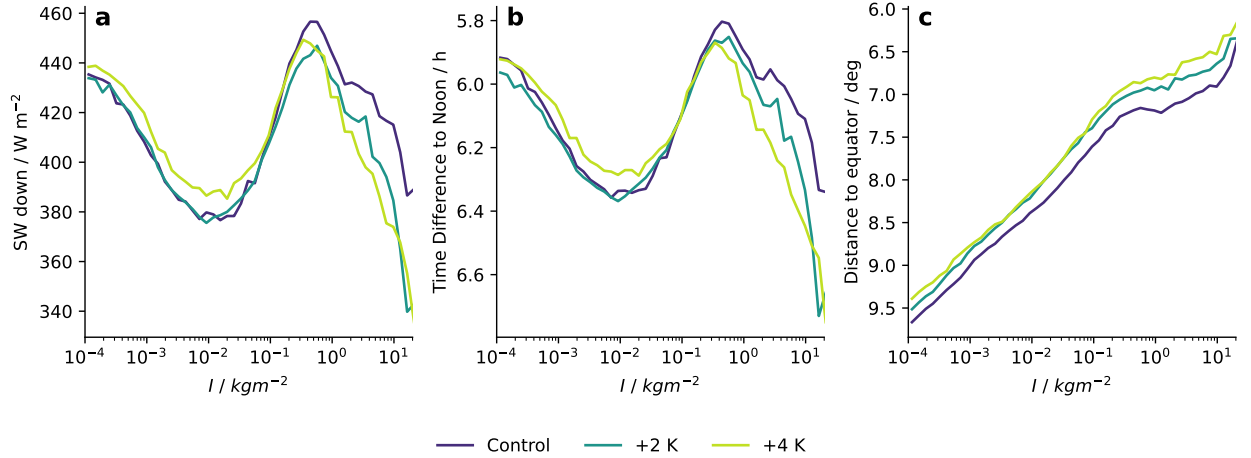


**Fig. S1** (a) Incoming SW radiation, (b) time difference to noon and (c) distance to the equator binned by ice water path ( $I$ ).

## 19 S2 Constant Ozone Simulation

20 To test the influence of the unrealistic assumption of ozone remaining constant on pressure levels despite  
 21 surface warming that is made within most GCMs, we conduct an additional +4 K simulation. For this  
 22 simulation, we prescribe the ozone from the control simulation rather than simulating ozone interactively.  
 23 We run three months of spin-up, followed by one month of simulation used for our analysis.

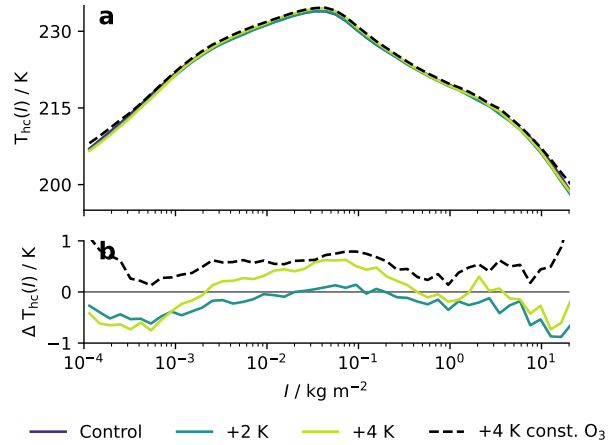


**Fig. S2** Like figure 3, but with results from the constant ozone run included.

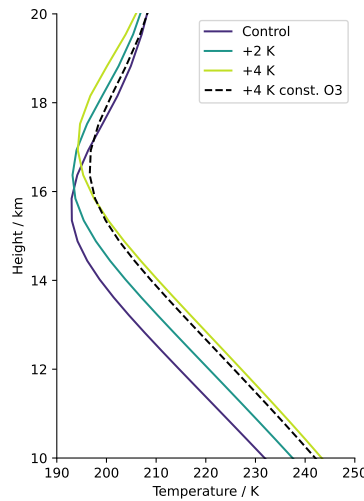


**Fig. S3** Mean clear-sky temperature profiles.

<sup>24</sup> **S3 Stability Iris**

<sup>25</sup> The static stability is increasing with surface warming as expected (Fig. S4b); however, this is partly cancelled  
<sup>26</sup> by an increase in radiative cooling due to lower density (Fig. S4a, Fig. S5). Therefore, changes in the  
<sup>27</sup> subsidence profiles and the convergence are small (Fig. S4c, d). This cancellation was also found by previous  
<sup>28</sup> studies, but seems more pronounced in our simulations [1].

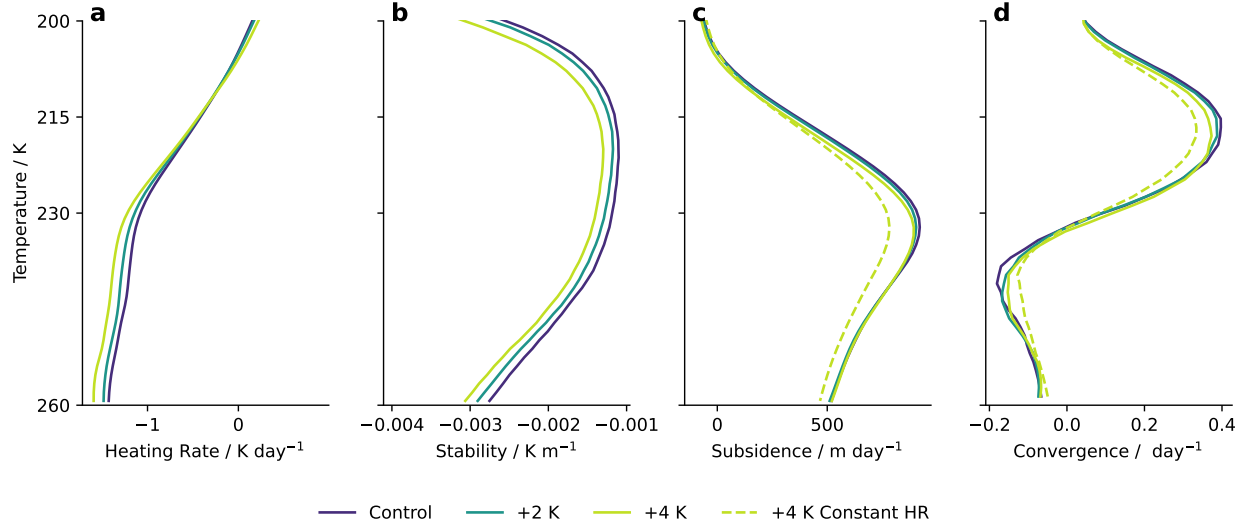


**Fig. S4** (a) Mean profiles within the clear-sky atmosphere of heating rate, (b) static stability, (c) radiatively driven subsidence and (d) horizontal convergence of radiatively driven subsidence. The dotted line in c and d shows results for the +4 K simulation with the heating rate fixed at the control profile.

29 **S4 Increase of Heating Rates**

30 Heating rates ( $Q$ ) are calculated as

$$Q = \frac{1}{\rho c_p} \frac{dF}{dz},$$

31 where  $\rho$  is density,  $c_p$  is specific heat capacity and  $F$  is the radiative flux. This implies that if the troposphere  
 32 extends upwards towards lower pressures with surface warming, heating rates in the upper troposphere  
 33 intensify due to the decrease in density if the flux convergence remains constant [2, 3]. Within our simulation,  
 34 this holds within clear-sky and cloudy regions, causing an amplification of heating rates (Fig. S5 and Fig. S6).

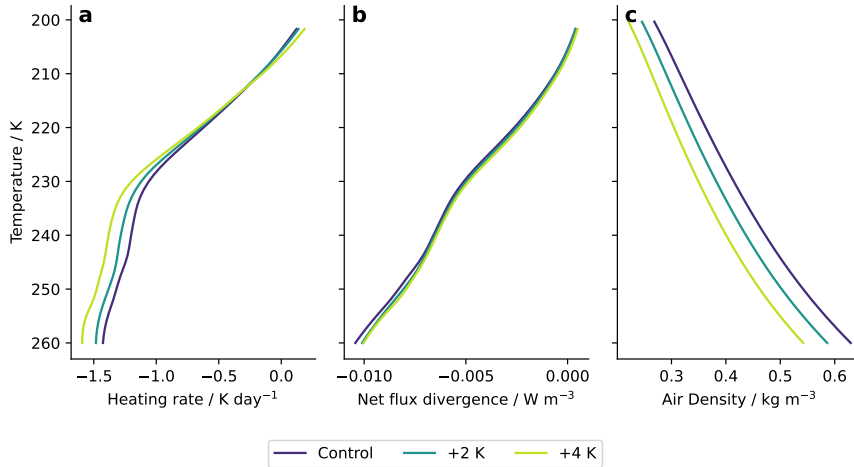


Fig. S5 (a) Clear-sky heating rate and (b) the contributions from the flux convergence and (c) density.

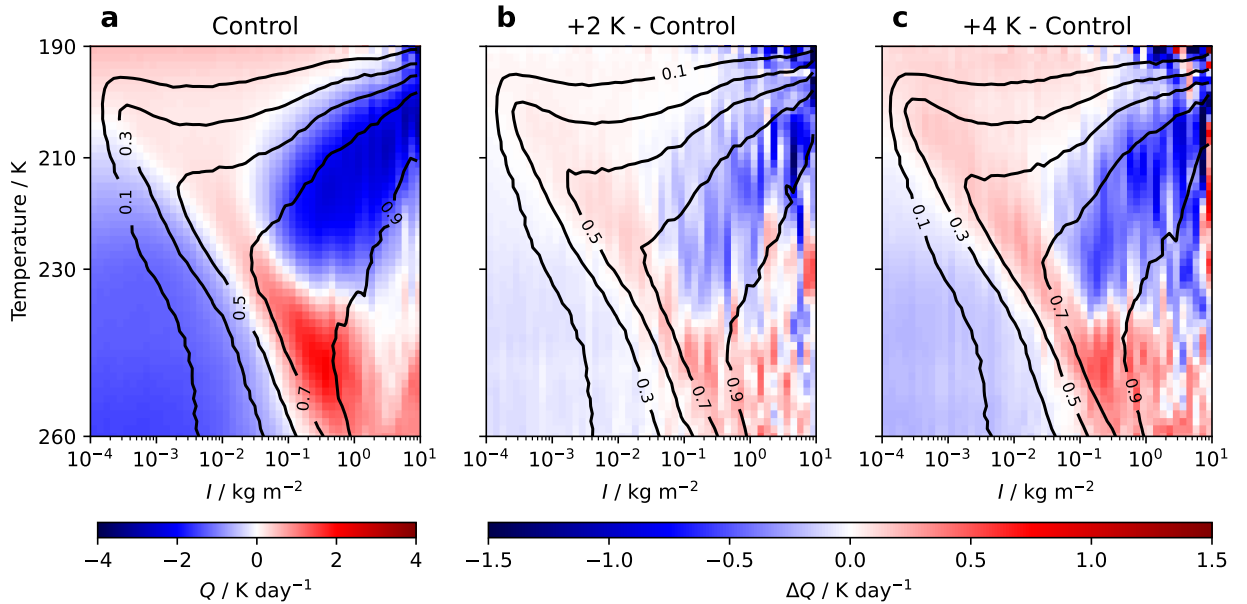


Fig. S6 (a) Radiative heating rate ( $Q$ ) binned by temperature and ice water path ( $I$ ) for the control run, (b, c) change in radiative heating rate ( $\Delta Q$ ) with respect to the control simulation.

35 We suspect that the intensification of cloud radiative heating might contribute to high-cloud thinning.  
 36 Thick high clouds with  $I > 3 \cdot 10^{-2}$  kg m<sup>-2</sup> experience a dipole of radiative heating, with heating at cloud  
 37 bottom and cooling above, whereas thinner clouds are heated throughout, which agrees with earlier studies

<sup>38</sup> [4, 5]. Both heating patterns become more pronounced with warming, which we suspect might affect the  
<sup>39</sup> cloud lifetime. A heating dipole was shown to destabilise the cloud layer and drive convection throughout,  
<sup>40</sup> leading to increased snow formation and precipitation [4]. An increased heating dipole in response to surface  
<sup>41</sup> warming might therefore decrease the lifetime of the affected clouds, which would explain their decreased  
<sup>42</sup> frequency of occurrence (Fig. 1e). On the other hand, radiative heating of thin high clouds has been shown  
<sup>43</sup> to loft and sustain them [5]. Hence, the increase in radiative heating of thin clouds might lead to a longer  
<sup>44</sup> lifetime, which would explain their increased frequency of occurrence.

## 45 S5 Testing Convergence of Statistics

46 To test whether three months of simulation are long enough to reach a statistically stable state, we investigate  
 47 the most fragile quantity of our analysis,  $\Delta P$ . When plotted with data from the first month, the first two  
 48 months and all three months of simulation,  $\Delta P$  shows convergence (Fig. S7). This proves that three months  
 49 of simulation are sufficient to reach a statistically stable state.

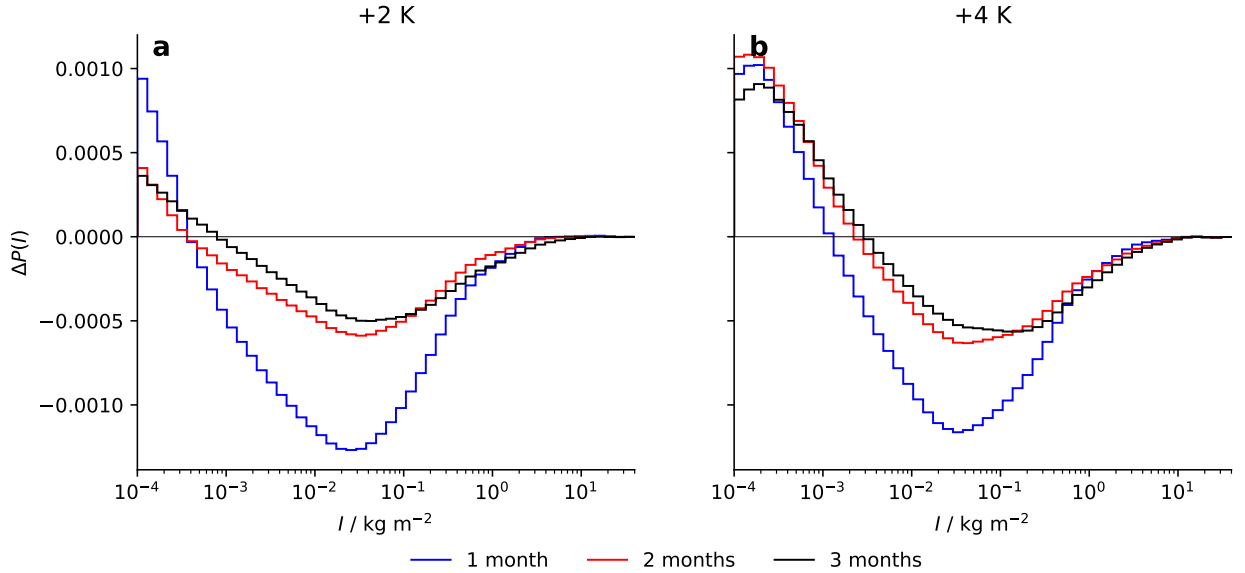


**Fig. S7** The difference between the ice water path frequency with respect to the control simulation ( $\Delta P(I)$ ) based on data from the first month, the first two months and all three months of the simulations for (a) the +2 K and (b) the +4 K simulation.

## 50 S6 Liquid Cloud Fraction Should Remain Constant with Warming

51 Liquid clouds are typically not connected to the frozen clouds at low  $I$ , but become increasingly connected  
 52 towards high  $I$ . According to our definition of high clouds, liquid clouds are part of the high clouds if  
 53 the liquid and frozen condensate within a column sufficiently overlap (Eq. 3). The transition from liquid  
 54 clouds being unconnected with the frozen clouds to liquid clouds being part of the high cloud occurs at  
 55  $1 \text{ kg m}^{-2} < I < 10 \text{ kg m}^{-2}$  (Fig. S8).

56 Without the tuning factor in Eq. 3, this transition would shift towards higher  $I$  with warming, which  
 57 would make the SW  $C(I)$  become less negative. This is a consequence of liquid clouds being more reflective  
 58 than the ocean surface. We regard this change in the SW  $C(I)$  and the associated feedback to be artificial  
 59 since it depends on subtle details of our definition of high clouds. Therefore, we introduce the tuning factor  
 60 to keep the liquid cloud fraction constant with warming.

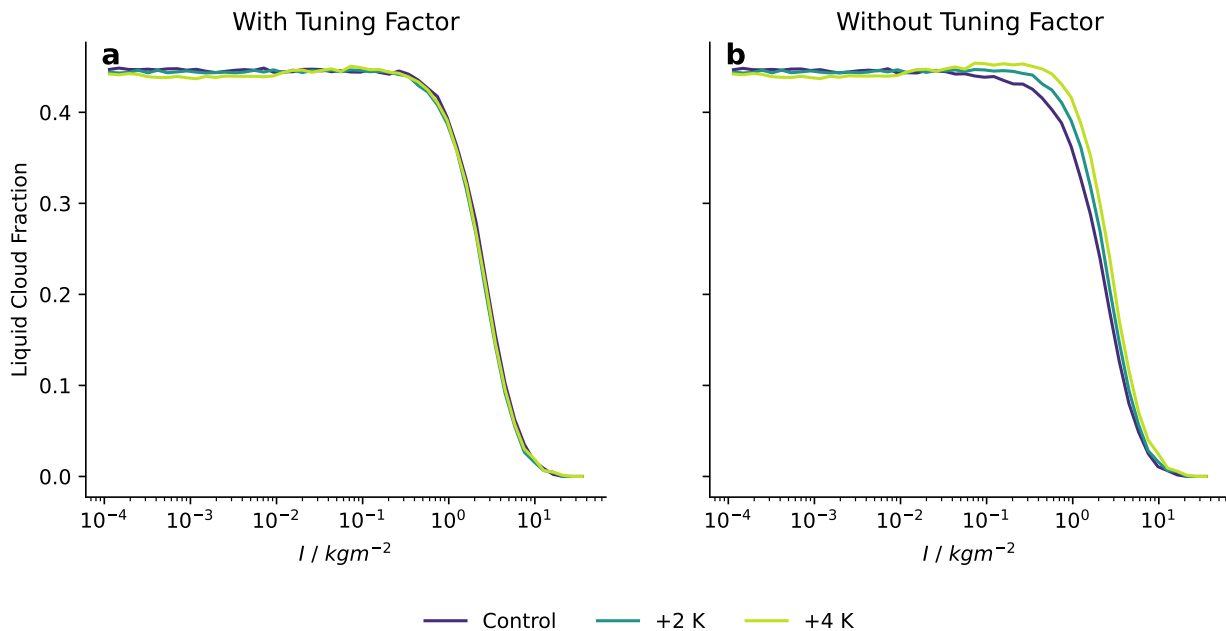


**Fig. S8** Fraction of liquid clouds with a liquid water path of more than  $10^{-4} \text{ kg m}^{-2}$  that are not part of high clouds (a) with and (b) without including the tuning factor designed to keep the liquid cloud fraction constant with warming.

## 61 References

62 [1] Bony, S., Stevens, B., Coppin, D., Becker, T., Reed, K.A., Voigt, A., Medeiros, B.: Thermodynamic  
 63 control of anvil cloud amount. *Proceedings of the National Academy of Sciences* **113**(32), 8927–8932  
 64 (2016) <https://doi.org/10.1073/pnas.1601472113> . Accessed 2023-06-01

65 [2] Gasparini, B., Mandorli, G., Stubenrauch, C., Voigt, A.: Basic Physics Predicts Stronger High Cloud  
 66 Radiative Heating With Warming. *Geophysical Research Letters* **51**(24), 2024–111228 (2024) <https://doi.org/10.1029/2024GL111228> . eprint: <https://onlinelibrary.wiley.com/doi/pdf/10.1029/2024GL111228>. Accessed 2025-01-22

69 [3] Jeevanjee, N., Fueglistaler, S.: On the Cooling-to-Space Approximation (2020) <https://doi.org/10.1175/JAS-D-18-0352.1> . Section: *Journal of the Atmospheric Sciences*. Accessed 2025-04-24

71 [4] Hartmann, D.L., Gasparini, B., Berry, S.E., Blossey, P.N.: The Life Cycle and Net  
 72 Radiative Effect of Tropical Anvil Clouds. *Journal of Advances in Modeling Earth  
 73 Systems* **10**(12), 3012–3029 (2018) <https://doi.org/10.1029/2018MS001484> . eprint:  
 74 <https://onlinelibrary.wiley.com/doi/pdf/10.1029/2018MS001484>. Accessed 2023-06-01

75 [5] Gasparini, B., Sokol, A.B., Wall, C.J., Hartmann, D.L., Blossey, P.N.: Diurnal Differences in Tropical  
76 Maritime Anvil Cloud Evolution. *Journal of Climate* **35**(5), 1655–1677 (2022) <https://doi.org/10.1175/JCLI-D-21-0211.1> . Publisher: American Meteorological Society Section: *Journal of Climate*. Accessed  
77 2023-11-16  
78